IEEE Access
Multidisciplinary | Rapid Review | Open Access Journal

Received July 19, 2019, accepted July 25, 2019, date of publication July 29, 2019, date of current version August 13, 2019.

Digital Object Identifier 10.1109/ACCESS.2019.2931704

Design of a Short-Circuit Detection Intelligent Release Using Discrete Wavelet Algorithm

GUANGHAI BAO[1,2], FENG ZENG[1,2], AND HUAIPING SUN[3]

[1]College of Electrical Engineering, Fuzhou University, Fuzhou 350108, China
[2]Fujian Key Laboratory of New Energy Generation and Power Conversion, Fuzhou 350108, China
[3]Nanan Power Supply Bureau of State Grid, Nanan 362300, China

Corresponding author: Guanghai Bao (19428733@qq.com)

ABSTRACT The short-circuit faults are one of the inevitable faults types in the power system. The frame circuit breaker can quickly break the transmission lines in case of the short-circuit faults to achieve the purpose of protecting the power system. At present, the method for detecting the short-circuit faults in the low-voltage distribution system by the intelligent release in the frame circuit breaker is mostly the rate of change of current or the effective value of current. Detection of the short-circuit faults by the rate of change of current has poor anti-interference ability. Detection of the short-circuit faults by the effective value will take a long time. In order to shorten the short-circuit fault detection time of the intelligent release, this paper proposes the wavelet packet decomposition as the short-circuit fault detection algorithm of the intelligent release. The multi-scale wavelet algorithm has a certain ability to filter white noise, and the singular value of the detail decomposition can be used to fast detection of the short-circuit faults when the short circuit occurs, which can shorten the detection time of the short-circuit faults. The results of the authoritative institutional tests prove that the intelligent release designed in this paper can detect the fault characteristics and send out the tripping signal within 0.5 ms after the short-circuit faults occur. The method proposed in this paper can be used in the low-voltage distribution system, as well as in medium-voltage and high-voltage situations to detect the short-circuit faults.

INDEX TERMS Short-circuit faults, intelligent release, wavelet packet decomposition, fast detection, authoritative institutional tests.

I. INTRODUCTION

The short-circuit faults are one of the inevitable faults types in the power system, where the single-phase short-circuit is the majority and the three-phase short-circuit is the least, but the damage of the latter is the most serious [1]–[3]. Therefore, the transmission lines, where the short-circuit fault occurs, should be broken quickly, which is beneficial to improve the stability of the power system operation [4]–[6]. The frame circuit breaker is one of the most important control and protection devices in the power system, and it has a wide range of applications [7], [8]. The intelligent release is the core control component of the frame circuit breaker. Its performance affects the overall performance of the frame circuit breaker and is also a guarantee for the safe operation of the power system [9], [10]. If it takes a long time for the intelligent release to detect the short-circuit faults, the characteristic of the current-limiting of the frame circuit breaker will be affected. With the development of the power system, more and more fast detection is required.

Reference [11] designs an intelligent release and uses TMS320VC5402 as the microprocessor, which has the functions of measuring, tripping and automatic reclosing. The rate of change of current can be used as the criterion of the short-circuit faults, which is proved by experiments. The rate of change of current method is simple, which can quickly detect short-circuit faults when applied to microprocessors, but it is sensitive to interference in the transmission lines, which easily causes misjudgment by interference. Reference [12], [13] use the cubic criterion method to judged whether a short-circuit fault has occurred. The principle of the cubic criterion is based on the instantaneous value of the short-circuit current and the rate of change of current. The second derivative of the current added to the Locus curve is used to judge faults comprehensively. Experiments show that this method can judge the short-circuit faults in a short time, but it does not have enough filtering function and anti-interference ability. What is more, the algorithm is more

The associate editor coordinating the review of this manuscript and approving it for publication was Francesco Tedesco.

This work is licensed under a Creative Commons Attribution 4.0 License. For more information, see http://creativecommons.org/licenses/by/4.0/

complex and difficult to be implemented on a microprocessor. Reference [14] develops an intelligent controller based on the dual-processor structure of DSP and ARM, which has the functions of measurement, protection, control, and communication. By calculating whether the effective value of the sampling current exceeds the set threshold, the short-circuit faults can be identified. The RMS algorithm is easy to be implemented on a microprocessor. However, the disadvantage of the algorithm is that it takes a long time to identify faults, and it needs a certain time to make a judgment after the short-circuit faults occur. It can not realize fast judgment of the short-circuit faults.

Reference [15] designs an early detection device for the short-circuit faults of the low-voltage distribution system based on TMS320F2812 DSP, which utilizes the singularity recognition and filtering function of wavelet packet decomposition to obtain the corresponding components through multi-scale detail decomposition and smoothing decomposition. The fourth scale detail decomposition component (cd4) is used as the criterion of the short-circuit faults. It is proved by experiments that the prototype can detect short-circuit faults within 0.2ms at the most fault phase angles, but the detection time will be longer at some fault phase angles of short-circuit current. For example, it takes 1.32ms for the device to detect the short-circuit faults with 150 degrees of the phase angle. Reference [16] uses dsPIC as the core processor to realize the preliminary application of the early detection model of the short-circuit faults, but there still has a problem that the detection time of the partial phase angle of short-circuit current is too long.

In view of the shortcomings of the current detection methods, to shorten the time of detecting short-circuit faults by the release, this paper designs an intelligent release and proposes to apply the early detection technology, which is the wavelet packet decomposition algorithm, to the short-circuit fault detection of the intelligent release. The detail decomposition component of the fourth scale detail decomposition components (dd5) is used as the criterion of the short-circuit faults. The purpose is to shorten the time of detecting the short-circuit faults less than 0.5ms within the full phase angle. At the same time, it can provide effective protection for overload faults in transmission lines. The device has a certain anti-interference ability so that it can quickly and reliably break the protected transmission lines when the short-circuit and overload occur. The method proposed in this paper can be used in a frame circuit breaker of the low-voltage distribution system, as well as in medium-voltage and high-voltage situations to detect the short-circuit faults. Most importantly, the device is confirmed that it can achieve overwhelmingly short detection in National Quality Supervision and Testing Center for Low-voltage Switching Device.

In section two, the current waveform of the short-circuit fault is analyzed to find a suitable identification algorithm. In section three and section four, the hardware and software parts of the intelligent release system based on the early detection technology of the short-circuit faults are introduced.

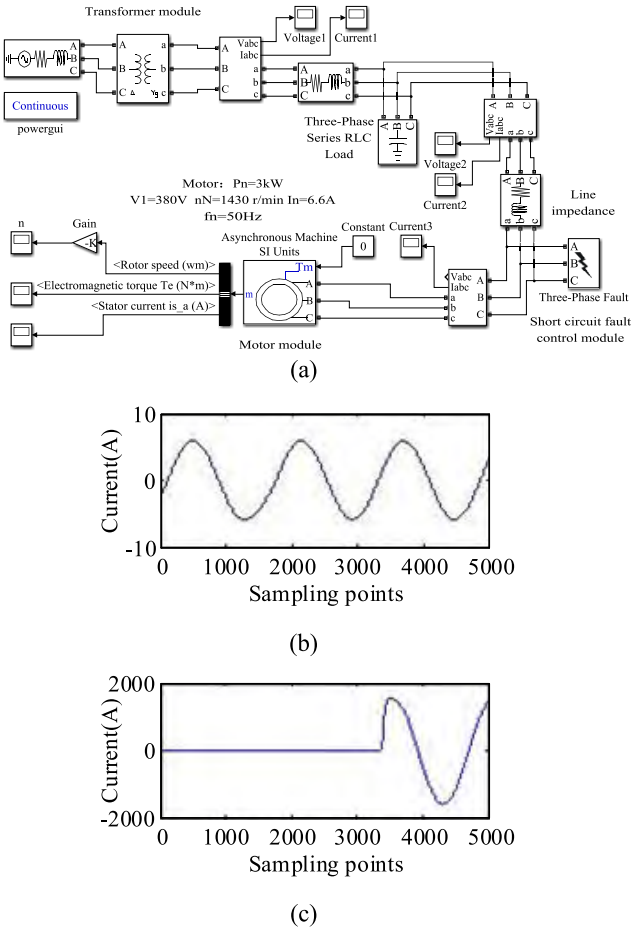

FIGURE 1. Simulation experiment platform and current waveform. (a) the Simulation experiment platform. (b) the current waveform under normal operation without the short-circuit fault. (c) the current waveform of the short-circuit fault.

In section five, it presents the test waveforms and the detection time of the intelligent release prototype. The authoritative test results show that the intelligent release using the early detection technology of short-circuit current can detect the short-circuit fault current in the full phase angle within 0.5ms and complete the tripping action.

II. SIMULATION ANALYSIS OF THE SHORT-CIRCUIT FAULT WAVEFORM

To analyze the current waveform of the short-circuit faults for finding a suitable identification algorithm, the current waveforms under normal and the short-circuit fault operation are obtained through using a Simulink simulation platform. The Simulink simulation platform is shown in Fig. 1a. The current waveform under normal operation without the short-circuit fault is shown in Fig. 1b and the current waveform under the short-circuit fault is shown in Fig. 1c.

Through the time domain analysis of the two waveforms, it can be seen that the method of calculating the RMS of the periodic current can better judge whether the collected current waveform has the characteristics of the faults. The RMS algorithm can be used as a criterion to judge whether

the short-circuit fault occurs in the transmission lines. However, the precondition of calculating the RMS of the current is to sample a complete period of the current data before calculating the RMS, which delays the detection time of the short-circuit faults. Therefore, it takes a long time to judge short-circuit fault by calculating the RMS of current, which is not conducive to practical application.

Compared with the current waveform in normal operation, the instantaneous rate of change of the current waveform is larger when the short-circuit faults occur. The method which is the rate of change of current can also judge whether short-circuit fault occurs. However, due to the influence of external electromagnetic interference, the current waveform will be mixed with high-frequency spike burrs in the actual normal electrical circuit. The method of calculating the instantaneous rate of change of current to identify the short-circuit faults will cause misjudgment. Therefore, it is not practical to calculate the instantaneous change rate of current.

In view of the shortcomings of the current detection methods, this paper proposes to apply the early detection technology, the wavelet packet decomposition algorithm, to the short-circuit fault detection of the intelligent release. The detail decomposition component of the fourth scale detail decomposition components (dd5) is used as the criterion of the short-circuit faults. The multi-resolution analysis of wavelet is equivalent to decomposing the sampled signal layer by layer using high-pass and low-pass filters. The smoothing decomposition of wavelet packet decomposition is used to filter high-frequency noise interference, while the detail decomposition component of a certain scale is actually the differential magnification of the smoothing component of the previous scale, which shows that the detail decomposition component reflects the continuous signal being decomposed. The smoothed derivative not only reflects the change rate of the signal but also eliminates the influence of noise interference by smoothing decomposition. Because of this excellent characteristic, wavelet packet detail decomposition is often used to detect mutation signal [17].

Fig. 2 illustrates to apply wavelet packet decomposition algorithm to the current waveform under normal operation without short-circuit fault. The current waveform under normal operation without short-circuit fault is obtained by Simulink simulation. The wavelet packet decomposition is divided into the detail decomposition of fourth scale detail decomposition components.

As can be seen from Fig. 2, the absolute values of detail components at each scale are relatively small when there is no obvious mutation point in the input signal. There are some abrupt changes in the detail components of each scale in the graph because the variable step size simulation is used in the simulation. Due to the abscissa of the figure is the sampling points, the time interval between some points is not equal, resulting in a small mutation. With the increase of decomposition scale, the magnitude of detail component increases, but the magnitude is still in a very small range.

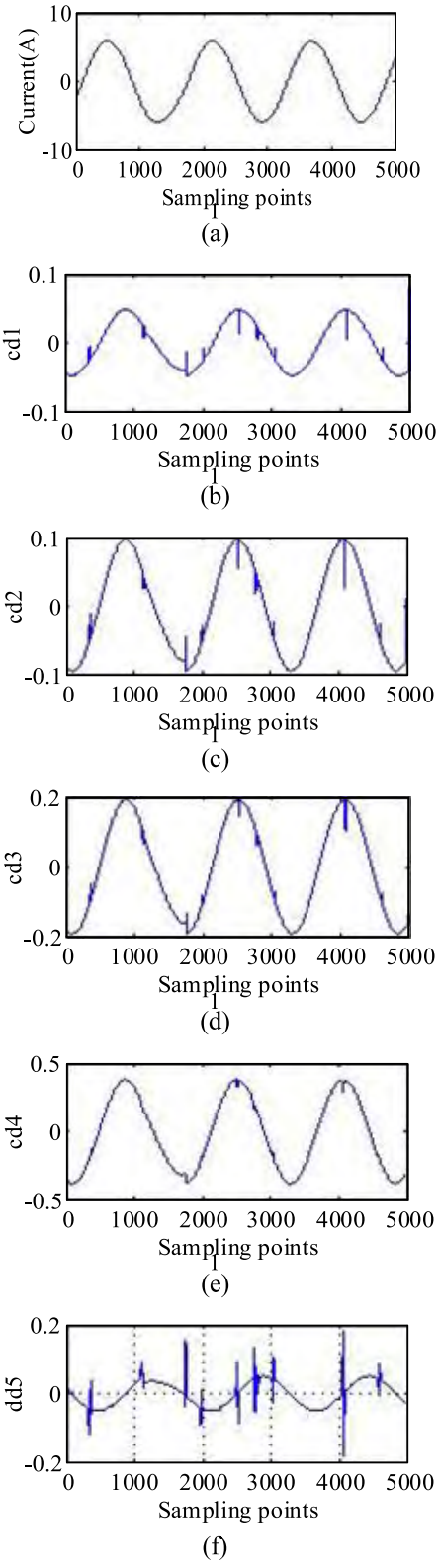

FIGURE 2. Detail decomposition of the sinusoidal current signal. (a) Original signal. (b) First-scale detail decomposition. (c) Second-scale detail decomposition. (d) Third-scale detail decomposition. (e) Fourth-scale detail decomposition. (f) Detailed decomposition of fourth-scale detail decomposition components.

Fig. 3 shows the waveform of detailed decomposition of signal with sudden change point. The decomposition scale is the same as that of Fig. 2. The input signal is the short-circuit current waveform simulated by Simulink.

As can be seen from Fig. 3, the waveform obtained by wavelet packet detail decomposition will have a peak when the input signal contains an abrupt point. The absolute value of this peak is much larger than that of the detail decomposition of the normal sinusoidal signal, and the peak will become larger and larger with the increase of the decomposition scale. Its peak value is close to 1000. This feature is very suitable for effectively and quickly detecting the short-circuit faults.

III. HARDWARE DESIGN OF INTELLIGENT RELEASE

The hardware structure block diagram of the intelligent release is shown in Fig. 4. The hardware part is mainly composed of two parts: the control part and the human-computer interaction part.

The control part includes the following modules: the double power supply module, the signal processing circuit, the signal comparison circuit, the pulse width detection circuit, the tripping control circuit, and the MCU with its peripheral circuits. The double power supply module is composed of a fast saturable power supply circuit and a power frequency voltage conversion circuit. The power which is obtained from the fast saturable transformer is supplied to the intelligent release. When the intelligent release works normally, the fast saturable power supply offers power to each module of the intelligent release. When the MCU sends out the tripping signal to break the transmission lines, the fast saturable power supply will be replaced with the power frequency power to continue to supply power to each module of the intelligent release, so as to ensure the stability and reliability of the power supply. The signal processing circuit is to elevate the original voltage signal to the one that can be recognized by the MCU.

The human-computer interaction part includes the following modules: the matrix key circuit, the digital display and its drive circuit, the LED lamp and its drive circuit. The matrix key circuit is used to set various electrical parameters, and each electrical parameter is displayed more intuitively through digital display and LED lamp to guide operation.

The intelligent release designed in this paper needs to select an MCU with a large number of pins, a high maximum frequency of the system, and a high precision of AD. The MCU selected in this paper is the PIC32MZ0512EFF064 produced by American Microchip Technology Incorporated. The chip has excellent performance. The system frequency of the chip is up to 200MHz, the pin number of the chip is 64, and it contains 6 AD sampling circuits. It meets the requirements of the chip selection in this paper.

The current in the transmission lines is coupled to the secondary side through the Rogowski coil. The voltage signal on the secondary side of the Rogowski coil is processed by the signal processing circuit, which can be identified and judged by MCU. When MCU identifies the short-circuit fault or overload, it sends out tripping signal to the tripping control circuit for driving the flux converter, which breaks the fault transmission lines. The hardware tripping module is

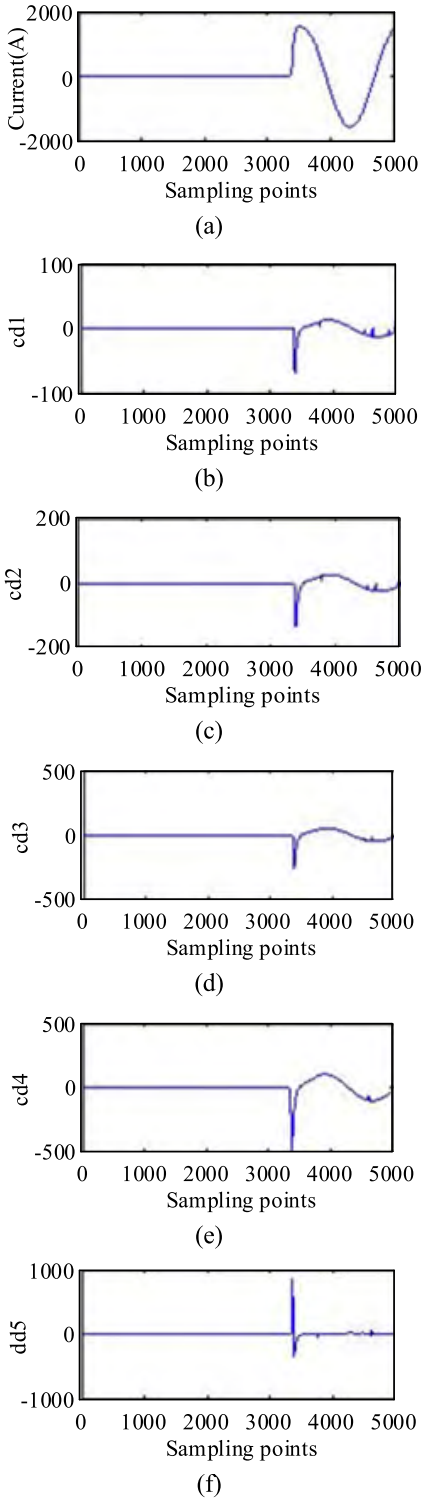

FIGURE 3. Detail decomposition of short-circuit current signal. (a) Original signal. (b) First-scale detail decomposition. (c) Second-scale detail decomposition. (d) Third-scale detail decomposition. (e) Fourth-scale detail decomposition. (f) Detailed decomposition of fourth-scale detail decomposition components.

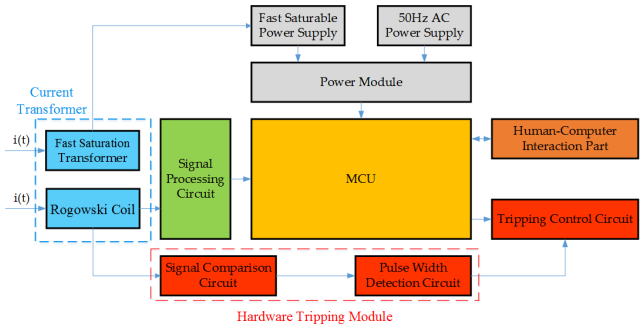

FIGURE 4. The hardware structure of the intelligent release.

FIGURE 5. The current transformer.

used as the backup protection function, in order to increase the reliability of the intelligent release. The voltage signal of the secondary side of the Rogowski coil is processed by the signal comparison circuit. When the voltage signal is above the set threshold, the signal comparison circuit sends out the tripping level to break the fault transmission lines.

A. CURRENT TRANSFORMER

The intelligent release designed in this paper is mainly used in the low-voltage frame circuit breakers. The current signal in the frame circuit breaker is transformed into a small voltage signal through the current transformer. The current transformer is shown in Fig. 5.

The current transformer is with a ratio of 1500A/100mV and has two outputs. One is the output of the Rogowski coil. The Rogowski coil is a circular coil wounded evenly on non-ferromagnetic material, which is not easy to cause saturation. It is used as sampling current signal. The other is the output of the coil wounded around the iron core, called the fast saturation transformer, which is used to absorb energy.

B. SIGNAL PROCESSING CIRCUIT

Because the selected MCU can only identify positive voltage and the voltage signal induced by the current transformer contains a negative part, the voltage signal needs to be raised by the signal processing circuit, and finally converted to the range from 0 to 3.3V voltages that the MCU can identify.

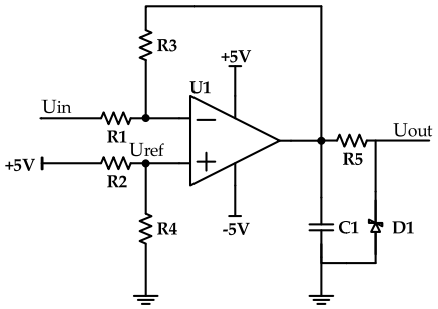

FIGURE 6. The signal processing circuit.

The signal processing circuit is a voltage lifting circuit with an operational amplifier as its core. Its working principle is to use the virtual short and virtual break of the operational amplifier to achieve the purpose of voltage lifting. A 3.3V zener diode D1 is used to prevent damage to the MCU when the voltage is too high.

The schematic diagram of the signal processing circuit is shown in Fig. 6.

According to the virtual short and virtual break, the formula for calculating the output voltage of the signal lifting circuit is as follows:

$$\begin{cases} U_{out} = \dfrac{R3}{R1} \times (U_{ref} - U_{in}) + U_{ref} \\ U_{ref} = \dfrac{5 \times R4}{R2 + R4} \end{cases} \tag{1}$$

where U_{in} is the input voltage, U_{ref} is the reference voltage at the non-inverting input of the operational amplifier, U_{out} is the output voltage after lifting.

C. TRIPPING MODULE

In addition to the tripping signal which can be produced by MCU, the hardware tripping module can also produce it as the backup protection to prevent the MCU from failing to break the line when the faults occur, which is composed of a signal comparison circuit, a pulse width detection circuit, and a tripping control circuit.

The signal comparison circuit is a voltage comparison circuit with a voltage comparator as its core. Each phase consists of two circuits. One is a positive voltage comparison and the other is negative voltage comparison. The signal comparison circuit is that the analog voltage induced by the current transformer is used as the input of the voltage comparison circuit to judge whether the action value is reached or not. The schematic diagram of the signal comparison circuit is shown in Fig. 7. U_{in} is the voltage analogue induced by the current transformer, and U_{out} is the tripping signal.

The formula for setting the positive voltage threshold is as follows:

$$U_{ref+} = \frac{5 \times R10}{R9 + R10} \tag{2}$$

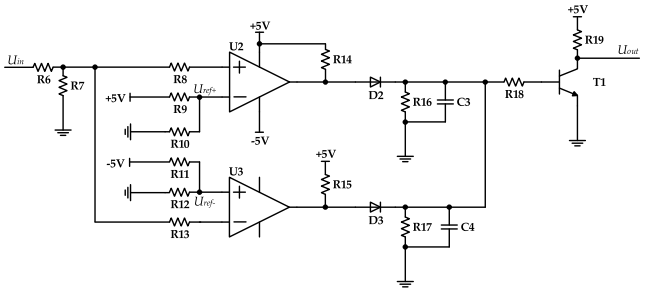

FIGURE 7. The signal comparison circuit.

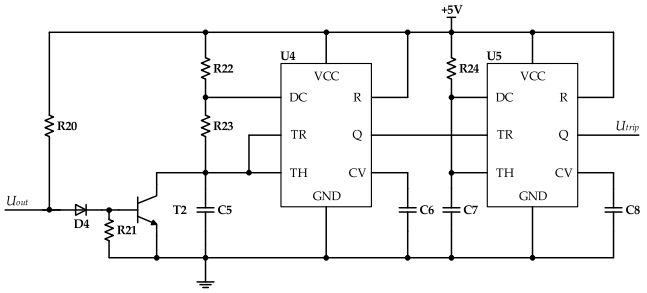

FIGURE 8. The pulse width detection circuit.

The formula for setting the negative voltage threshold is as follows:

$$U_{ref-} = \frac{-5 \times R12}{R11 + R12} \tag{3}$$

When the positive voltage is greater than U_{ref+} or the negative voltage is less than U_{ref-}, the voltage comparator outputs a voltage of about 5V, which makes the triode T1 turn on, and the collector of the triode is pulled from a high level to a low level. The duration of the low level is determined by the time when the input signal exceeds the set value.

The pulse width detection circuit consists of two 555 chips, which are U4 and U5. The output of the U4 is connected with the input of the U5. U_{out} is the output of the signal comparison circuit, and U_{trip} is the signal for driving the tripping control circuit to work. The schematic diagram of the pulse width detection circuit is shown in Fig. 8.

When the level of U_{out} changes from high value to low one, +5V starts to charge C5 through R22 and R23. When the voltage of both ends of C5 reaches 2Vcc/3, the charging will finish and the charging time is τ_1. The formula (4) for τ_1 is as follows:

$$\tau_1 = 1.1 \times (R22 + R23) \times C5 \tag{4}$$

The level of Q-pin of U4 changes from high value to a low value, which triggers U5 to work, and the output of U5 shows a pulse of time length τ_2. The formula (5) for τ_2 is as follows:

$$\tau_2 = 1.1 \times R24 \times C7 \tag{5}$$

The purpose of the pulse width detection circuit is to filter out the narrow pulse of low level caused by external interference. If the width of this pulse is less than τ_1, U5 will not output a high-level pulse. Only when the width of the low-level pulse is greater than τ_1, U5 can output a high-level pulse,

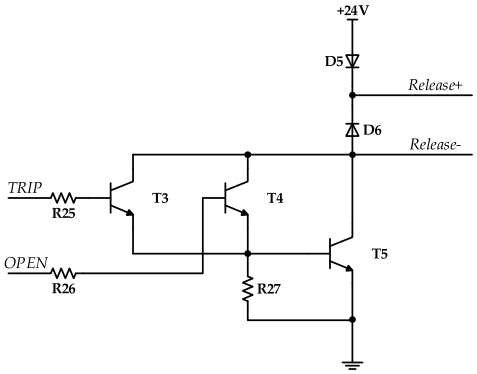

FIGURE 9. The tripping control circuit.

which can avoid the misjudgment caused by interference and improves the reliability of the intelligent release.

The tripping control circuit is a Darlington transistor consisting of two triodes, which is used to control the conduction of the flux converter. The *TRIP* input of the tripping control circuit is connected to the output of the pulse width detection circuit as hardware tripping. The *OPEN* input of the tripping control circuit is connected to the MCU as the software tripping. A flux converter is connected between the *release*+ output and the *release*− output of the tripping control circuit. When the flux converter is energized, the corresponding mechanism moves to make the frame circuit breaker trip. The schematic diagram of the tripping control circuit is shown in Fig. 9.

The *OPEN* input is low level when the MCU does not send out the tripping signal. The triode T4 and the triode T5 are cut-off. The flux converter and the power supply do not constitute a loop circuit. When the MCU sends out the tripping signal, the *OPEN* input of the tripping control circuit becomes a high level. The T4 is conducting so that the T5 is also conducting. Then, the flux converter can work to drive the release action. When the *OPEN* input becomes low level again, the T4 and the T5 turns cut-off. The flux converter can discharge its energy through the diode D6 to prevent overvoltage and damaging the circuit and components. The tripping signal from the pulse width detection circuit and the tripping signal from the MCU are controlled by two triodes T3 and T4 respectively, and they do not affect each other.

Through the above circuit design, the PCB board of the intelligent release prototype can be determined. The prototype is shown in Fig. 10.

IV. SOFTWARE DESIGN OF THE INTELLIGENT RELEASE

A. ESTABLISHMENT OF MATHEMATICAL MODEL OF WAVELET PACKET DECOMPOSITION ALGORITHM

The wavelet packet decomposition algorithm decomposes the signal to get the high-frequency detail components and the low-frequency smooth components [18], [19]. The high-frequency detail component represents the fault signals, and the low-frequency smooth component is the normal signals [20]. The short-circuit faults are identified by comparing detail components with pre-set thresholds.

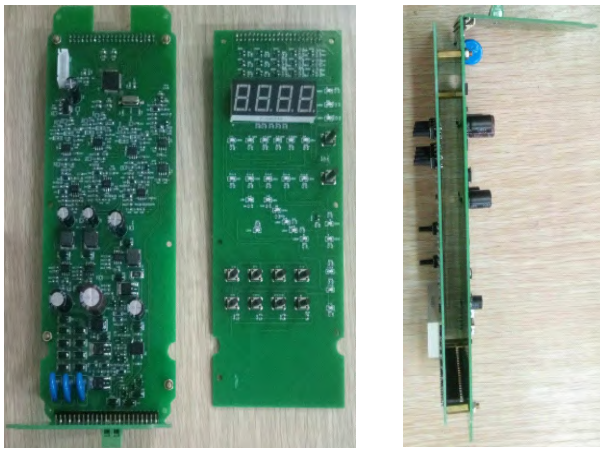

(a) (b)

FIGURE 10. Physical drawing of intelligent release prototype. (a) Top view of the prototype. (b) Side view of the prototype.

The recursion formula of Mallat algorithm is shown in Formula 6 [21], [22].

$$\begin{cases} S_{2j}f(n) = \sum_k h_k S_{2j-1}f(n-2^{j-1}k) \\ W_{2j}f(n) = \sum_k g_k S_{2j-1}f(n-2^{j-1}k) \end{cases} \tag{6}$$

where j is the decomposition scale and $j > 0$, h_k is the coefficients of low-pass filters, g_k is the coefficients of high-pass filters, $S_{2j}f(n)$ is the smoothing component on the jth decomposition scale, $W_{2j}f(n)$ is the detail component on the jth decomposition scale.

Because the multi-resolution analysis of wavelet transform only decomposes the smooth components step by step, the frequency domain resolution of the corresponding wavelet basis function becomes better and the time domain resolution becomes worse as the decomposition scale increases. Therefore, in order to solve the disadvantage of poor resolution of wavelet transform in high frequency band of signal, this paper introduces a wavelet packet decomposition algorithm based on wavelet analysis, that is, further decomposition of detail components in the fourth scale, so that the detail components obtained by decomposition can have sufficient resolution in both time and frequency domains. The fast recursion formula of the wavelet packet decomposition algorithm is shown in Formula 7 [23].

$$\begin{cases} S_{2^j}^{(2p)}f(n) = \sum_{k=-1}^{2} h_k S_{2^{j-1}}^{(p)}f(n-2^{j-1}k) \\ W_{2^j}^{(2p+1)}f(n) = \sum_{k=0}^{1} g_k S_{2^{j-1}}^{(p)}f(n-2^{j-1}k) \end{cases} (p \text{ is even number})$$

$$\begin{cases} S_{2^j}^{(2p)}f(n) = \sum_{k=-1}^{2} h_k W_{2^{j-1}}^{(p)}f(n-2^{j-1}k) \\ W_{2^j}^{(2p+1)}f(n) = \sum_{k=0}^{1} g_k W_{2^{j-1}}^{(p)}f(n-2^{j-1}k) \end{cases} (p \text{ is odd number}) \tag{7}$$

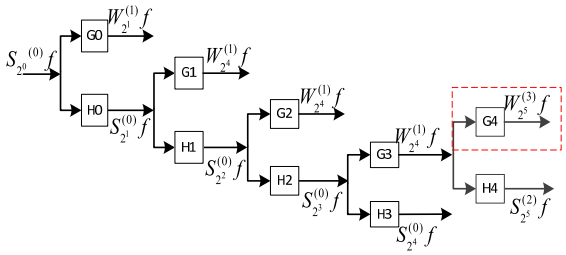

FIGURE 11. The schema of wavelet packet decomposition.

TABLE 1. The coefficients of low-pass and High-pass filters.

k	-3	-2	-1	0	1	2
h_k	0	0	1/8	3/8	3/8	1/8
g_k	0	0	0	-2	2	0

The schema of wavelet packet decomposition is shown in Fig. 11.

B-spline wavelet is a commonly used wavelet basis in engineering signal analysis. It is not only continuous but also symmetrical. The research shows that B-spline wavelet functions have the advantages of easy derivation and easy realization on MCU, and it has explicit analytical formulas. In addition, compared with other wavelet basis, B-spline wavelet has a better ability to filter noise and detect singularity of the abrupt signal [24]. Therefore, the derivative of a cubic B-spline function is chosen as the wavelet function. The coefficients of low-pass and high-pass filters are shown in Table 1 [25].

The coefficients of low-pass and high-pass filters of B-spline function are combined with Mallat fast recursion formula 7. Then, the concrete expression of cubic B-spline improved wavelet decomposition algorithm can be obtained.

Wavelet decomposition itself has a certain filtering function. The more decomposition layers are, the smoother the waveform will become and the less noise will be, but the amount of calculation will also be greatly increasing, which is not conducive to the realization in MCU. Therefore, in practical application, we should not only consider the filtering effect but also consider the operation speed of MCU.

B. INTEGRAL DESIGN OF INTELLIGENT RELEASE PROGRAM

The intelligent release designed in this paper can effectively protect the transmission lines from the short-circuit faults and overload. The wavelet packet decomposition algorithm is used to identify and judge whether the short-circuit fault occurs in the transmission lines. The thermal effect of overload current is recorded to judge whether overload occurs in the transmission lines.

Programming of the intelligent release includes wavelet packet decomposition for current signals, the effective value

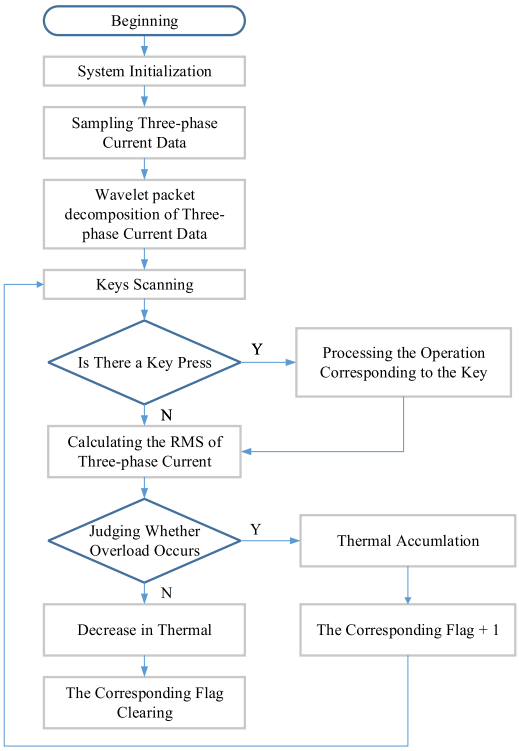

FIGURE 12. Flowchart of the main program.

calculating of three-phase current, keys scanning and fault identification.

The flowchart of the main program is shown in Fig. 12.

After initialization, the program starts to sample 46 points of each phase current data and then performs wavelet packet decomposition. The 46 points are sampled because more points will be lost with the increase of decomposition scale, and 45 points will be lost when signals are decomposed into the detail decomposition of fourth-scale detail decomposition, so at least 46 points can get a value of the detail decomposition of fourth-scale detail decomposition components.

After that, the program enters the loop body, which first scans whether there are keys pressed or not, and then processes them according to the scanning results. If there are keys pressed, the corresponding operation will be performed according to what key obtained. Then, the effective values of three-phase current are calculated according to the stored current data, and the set thresholds are used to judge whether overload occurs. If overload occurs, heat accumulation will be recorded, and if no overload occurs, the heat will be reduced to a small value. Then the program goes back to the key scan to form a loop.

The program of analog and digital sampling is completed in an interrupt service program. The interrupt service program mainly obtains the data of current in real-time and decomposed them by wavelet transform. Then the MCU judged whether the fault occurs in real-time, and sent out the trip signal if it happened.

C. PROGRAMMING OF WAVELET PACKET DECOMPOSITION ALGORITHMS

Wavelet decomposition is an algorithm applied to detecting the short-circuit faults in this paper. The noise is filtered by smoothing decomposition, and the eigenvalues of abrupt signals are obtained by detail decomposition. With the increase of the wavelet decomposition scale, some data of the original signals will be lost. To get the detailed decomposition component of fourth-scale detail decomposition components, at least 46 original data will be needed.

After the initialization of the main program of the intelligent release is completed, 46 points of each phase current data are collected and stored in the array IA[46], IB[46], and IC[46], respectively. Then the current data in the arrays are decomposed by wavelet transform. After decomposition, the detailed decomposition component of fourth-scale detail decomposition components is stored in variables W5A, W5B, and W5C, respectively. After that, the MCU carries out Array shift and wavelet decomposition once every sampling point is obtained. After decomposition, the absolute values of W5A, W5B, and W5C of the detailed decomposition component of fourth-scale detail decomposition components are compared with the corresponding thresholds respectively. If the value is larger than the threshold, the trip signal is sent out. Array shift means that when new data sampling is completed, they are stored in variables NewA, NewB, and NewC respectively. Remove the first data from the array IA[46], IB[46], and IC[46], and move the left data forward in turn. Then put the data of the variables NewA, NewB and NewC into the last element of the array so that the acquisition can achieve fast calculation. In order to achieve the purpose of real-time detection, the data processing of this point should be completed before the next sampling data arrives. The sampling frequency of the intelligent release designed in this paper is 20kHz, that is, the sampling time interval is 50us. After testing, the time of wavelet packet decomposition for new sampling points of three-phase current is about 35us, which meets the requirement under 200MHz working frequency of MCU. The time between the end of wavelet packet decomposition and the arrival of the next sampling data can be used to scan and process keys in the main program, and calculate the RMS of current.

After sampling 46 points of three-phase current data, the wavelet packet decomposition subprogram is used to decompose the three-phase current data. The software design of the three-phase wavelet packet decomposition algorithm is similar. This paper presents only the program design of the wavelet packet decomposition algorithm for phase A current data. The flowchart of the subprogram of wavelet packet decomposition for phase A current data is shown in Figure 13.

Where IA is the array name for the A phase current data storage array. S1A is the array name for the first-scale smoothing components storage array. S2A is the array name for the second-scale smoothing components storage array. S3A is the array name for the third-scale smoothing components storage array. W4A is the array name for the

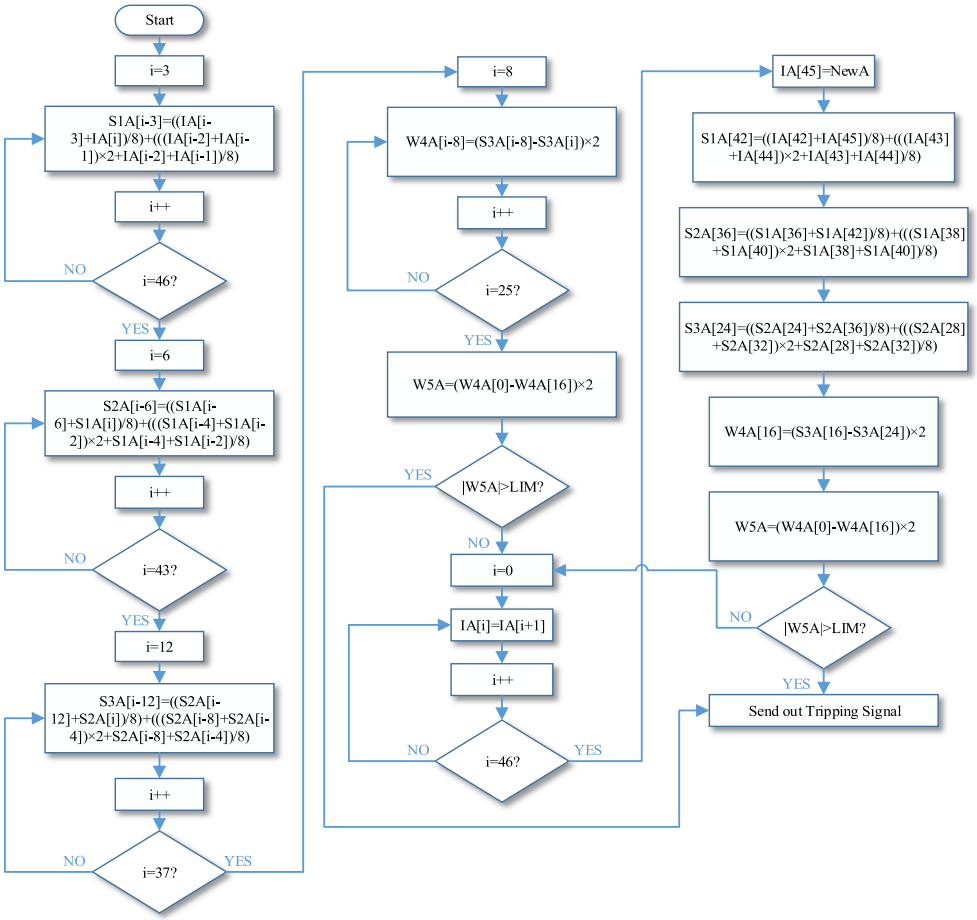

FIGURE 13. The flowchart of the subprogram of wavelet packet decomposition for phase A current data.

fourth-scale detail decomposition components storage array. W5A is the array name for the detailed decomposition component of fourth-scale detail decomposition components storage array. NewA is a variable that stores a new data sampled for phase A. LIM is a variable that stores the set threshold.

V. EXPERIMENTAL VERIFICATION

In this paper, the feasibility of the short-circuit faults protection scheme using early detection technology is verified by simulation experiments, practical experiments, and authoritative institutional tests.

A. SIMULATED SHORT-CIRCUIT FAULT EXPERIMENTS

The simulated short-circuit test uses Simulink software to build a simulation circuit model to simulate the short-circuit faults. The circuit model is shown in Fig. 14.

It simulates the circuit model in reality, and the three-phase fault control module and the motor module are added in the circuit. Because the starting current of the three-phase asynchronous motor is very large when it starts, it will produce a similar phenomenon to short-circuit fault current. Therefore, this experiment can also test whether there will be misjudgment in the starting process of the motor. The simulation software saves the current data corresponding to the simulation short-circuit fault, and the phase angle is simulated every 10 degrees. An arbitrary waveform generator (named Agilent 33522A) is used to generate a voltage signal from the corresponding current data. The intelligent release control board detects the voltage signal to judged whether a short-circuit fault occurs.

During the test, the signal generated by the waveform generator is connected to the intelligent release control board. When the fault is detected, the corresponding pin sends out a tripping signal and the waveform is recorded by an oscilloscope. Fig. 15 shows the waveform of the tripping signal and the short-circuit current waveform with the fault phase angle of 0 degree. The blue waveform is the short-circuit current signal, and the orange waveform is the tripping signal. The short-circuit current signal is lifted by an operational amplifier. Fig. 15 (b) is a waveform enlargement of Fig. 15 (a) at breaking time. Test results of partial fault phase angles from 0 to 170 degrees are shown in Fig. 15-18.

From Fig. 15 to Fig. 18, it can be seen that the intelligent release prototype can detect the short-circuit faults and send out tripping signals in a relatively short time. The detection time of the intelligent release prototype is 300us

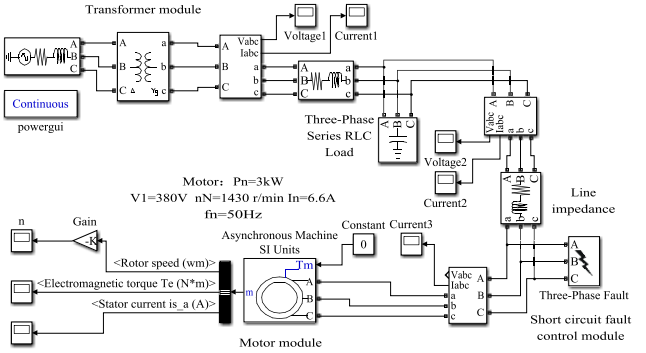

FIGURE 14. Simulated circuit diagram with a motor load.

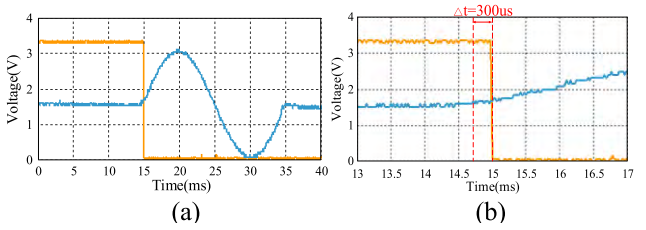

FIGURE 15. Detection time of short-circuit fault with a fault phase angle of 0 degree. (a) Short-circuit fault detection time waveform. (b) Waveform amplification diagram at breaking time.

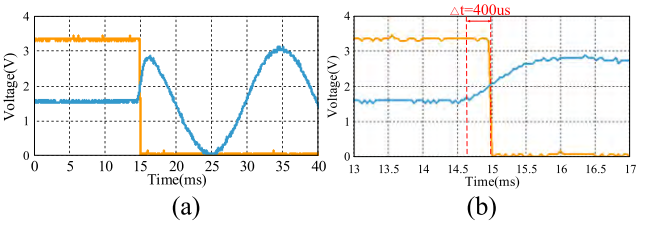

FIGURE 16. Detection time of short-circuit fault with a fault phase angle of 90 degrees. (a) Short-circuit fault detection time waveform. (b) Waveform amplification diagram at breaking time.

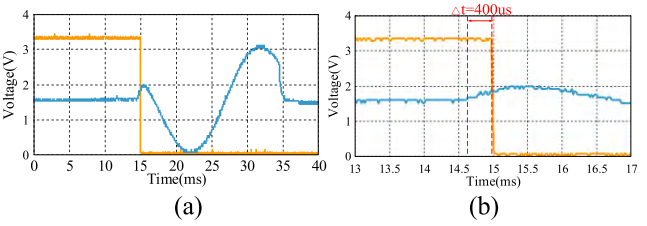

FIGURE 17. Detection time of short-circuit fault with a fault phase angle of 150 degrees. (a) Short-circuit fault detection time waveform. (b) Waveform amplification diagram at breaking time.

when the short-circuit fault occurs with the fault phase angle of 0 degree. The detection time of the intelligent release prototype is 400us when the short-circuit fault occurs with the fault phase angle of 150 degrees.

Table 2 shows the detection time of the short-circuit faults with fault initial phase angle of 0-180 degrees and the corresponding current per unit when the tripping signal is detected.

From Table 2, it can be seen that the intelligent release prototype with early fault detection technology can realize

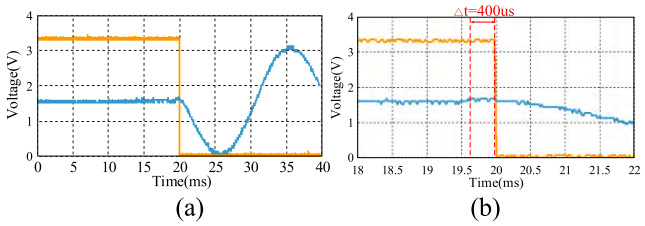

FIGURE 18. Detection time of short-circuit fault with a fault phase angle of 170 degrees. (a) Short-circuit fault detection time waveform. (b) Waveform amplification diagram at breaking time.

FIGURE 19. The experimental environment of distribution short-circuit system.

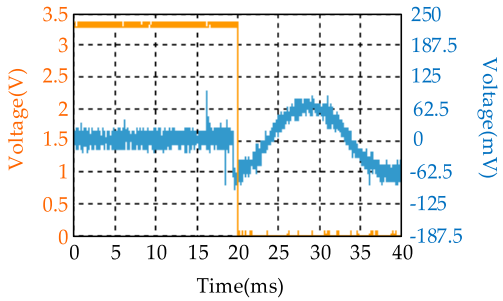

FIGURE 20. The experimental waveform of 30 degrees short-circuit current with fault phase angle.

early detection of short-circuit faults in the whole phase angle range. The detection time is between 200us and 400us and the short-circuit current is relatively small at this time, which can achieve early detection.

B. PRACTICAL SHORT-CIRCUIT FAULT EXPERIMENTS

The actual short-circuit experiment is completed by using the distribution short-circuit system, which consists of the distribution short-circuit overhead network, the distribution short-circuit power supply cabinet, the distribution short-circuit simulation cabinet and the distribution short-circuit control cabinet. When the short-circuit current is detected, the corresponding pins of the MCU send out the tripping signal and record the waveform by an oscilloscope. Overhead power network simulates transmission lines. The power supply cabinet is used to connect and disconnect the power supply.

TABLE 2. Experimental results of short-circuit simulation for initial phase angle of 0-180 degrees.

Fault Initial Phase Angle	0°	10°	20°	30°	40°	50°	60°	70°	80°
Detection time	300us	300us	280us	280us	280us	320us	320us	280us	280us
i* (t_0)	1.63	1.72	1.68	3.21	2.61	2.73	2.91	2.72	2.78
Fault Initial Phase Angle	90°	100°	110°	120°	130°	140°	150°	160°	170°
Detection time	400us	280us	280us	360us	360us	360us	400us	400us	400us
i* (t_0)	3.27	2.39	2.55	2.04	2.32	2.46	2.79	2.83	2.88

TABLE 3. Actual experimental results of 0-180 degrees fault initial phase angle short-circuit.

Fault Initial Phase Angle	0°	10°	20°	30°	40°	50°	60°	70°	80°
Detection time	360us	480us	400us	480us	440us	480us	400us	400us	500us
i* (t_0)	1.72	1.83	1.75	3.41	2.76	2.81	3.01	3.07	3.23
Fault Initial Phase Angle	90°	100°	110°	120°	130°	140°	150°	160°	170°
Detection time	400us	400us	400us	480us	440us	480us	480us	500us	500us
i* (t_0)	3.18	3.12	3.07	3.24	3.12	3.13	3.09	3.11	3.04

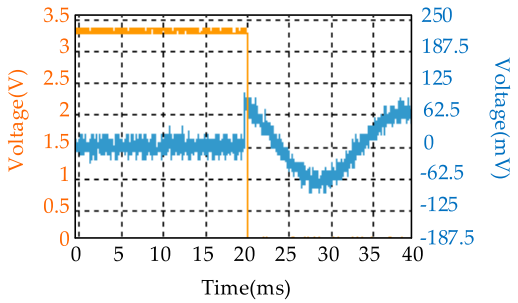

FIGURE 21. The experimental waveform of 60 degrees short-circuit current with fault phase angle.

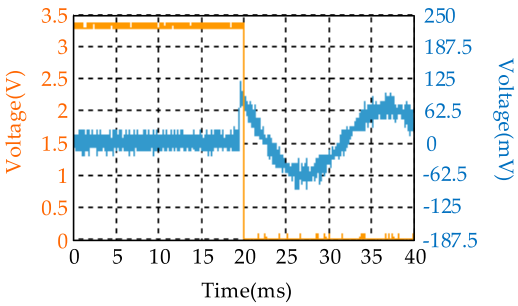

FIGURE 22. The experimental waveform of 90 degrees short-circuit current with fault phase angle.

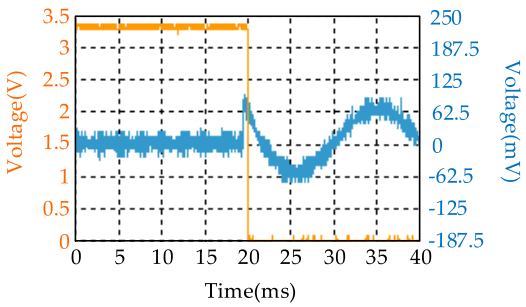

FIGURE 23. The experimental waveform of 120 degrees short-circuit current with fault phase angle.

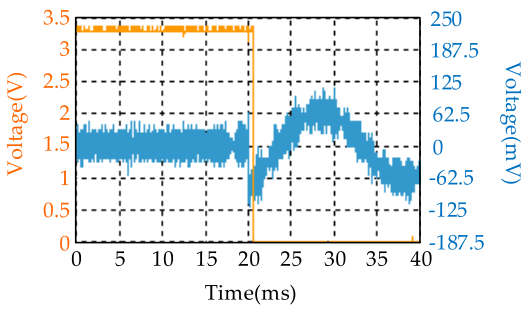

FIGURE 24. The experimental waveform of 150 degrees short-circuit current with fault phase angle.

The distribution short-circuit simulation cabinet is used to select short-circuit type and transmission lines (line diameter, length). The distribution short-circuit control cabinet is used to switch relays by on/off so as to control the occurrence of short-circuiting. It can output short-circuit current up to 2kA. The experimental environment is shown in Fig. 19.

Fig. 20-25 show the short-circuit current waveform and tripping signal waveform at different fault phase angles. The fault phase angles are 30 degrees, 60 degrees, 90 degrees, 120 degrees, 150 degrees, and 170 degrees, respectively. The blue waveform is the short-circuit current signal, and the orange waveform is the tripping signal. The blue ordinate

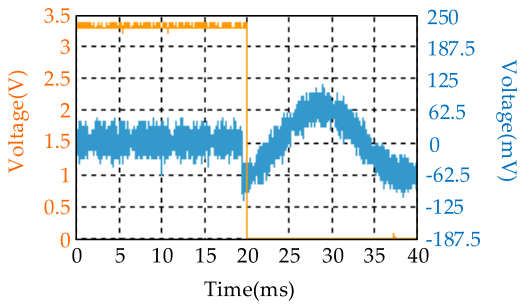

FIGURE 25. The experimental waveform of 170 degrees short-circuit current with fault phase angle.

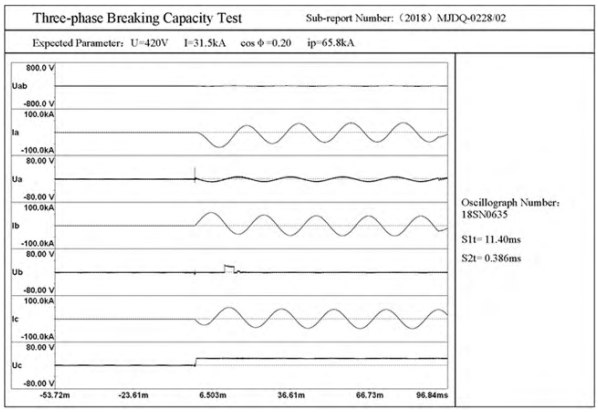

FIGURE 26. Test report chart of operation time of 30kA short-circuit current.

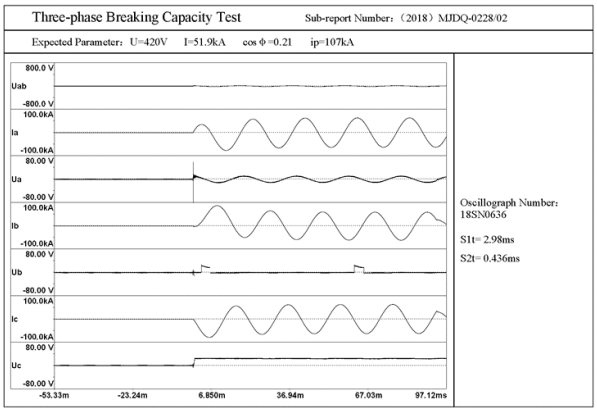

FIGURE 27. Test report chart of operation time of 50kA short-circuit current.

scale corresponds to the short-circuit current signal waveform. The orange ordinate scale corresponds to the tripping signal waveform. Because of the noise in the current signal, the waveform looks rough.

Table 3 shows the detection time of short-circuit faults with fault initial phase angle of 0-180 degrees and the corresponding current per unit when the tripping signal is detected. Because the short-circuit current is relatively small and the voltage induced by the transformer is relatively small in reality, only about 100mV, the sudden change degree of the short-circuit current is relatively small and the detection time is longer than the previous simulation experiment. But the short-circuit fault can still be detected within 0.5ms at the full phase angle, which verifies the feasibility of the early detection algorithm, which is applied to the hardware design of intelligent release.

C. AUTHORITATIVE INSTITUTIONAL TESTS

In order to test whether the intelligent release prototype with early detection technology meets the national standard of China. The prototype is taken to the National Quality Supervision and Testing Center for Low-voltage Switching Device for short-circuit fault testing and compared with an intelligent release which has a wide audience on the market. The tripping time of the devices are measured by applying 30kA and 50kA short-circuit current with an arbitrary phase angle. The experimental report is shown in Figs. 26 and 27.

Intelligent release S1 is an intelligent release proposed in other companies. Intelligent release S2 is an intelligent release prototype proposed in this paper. S1t is the time of detecting short-circuit faults by intelligent release S1. S2t is the time of detecting short-circuit faults by intelligent release S2. From the waveform diagram in the experiment report, it can be seen that when 30kA short-circuit current is applied, the tripping time of S1 is 11.4ms and that of S2 is 0.386ms. When 50kA short-circuit current is applied, the tripping time of S1 is 2.98ms and that of S2 is 0.436ms. From the comprehensive experimental data, it can be seen that when the short-circuit fault occurs on the transmission lines, the tripping time of the intelligent release prototype S2 proposed in the paper is much shorter than that of the intelligent release S1. The advantage of the intelligent release using early detection technology in identifying the short-circuit faults is obvious, which meets the requirements of National standards.

VI. CONCLUSION

This paper proposed the use of early detection technology as the short-circuit fault detection technology for frame circuit breakers, aiming at shortening the detection time of short-circuit faults for the intelligent release. Through the design of the hardware circuit and software program, an intelligent release is made. Through simulated short-circuit tests and actual short-circuit tests, the experimental results show that the prototype can detect the short-circuit faults within 0.2-0.5ms after the short-circuit faults with an arbitrary phase angle occur on the protected transmission lines, and the prototype can send out the tripping signal at the same time. The early detection of the short-circuit faults in the full phase angle range is realized, and the feasibility of applying the early detection algorithm to the hardware design of the intelligent release is verified. Most importantly, the intelligent release proposed in the paper passed the authoritative tests from the National Quality Supervision and Testing Center for Low-voltage Switching Device.

The method proposed in this paper can be used in a frame circuit breaker of the low-voltage distribution system, as well as in medium-voltage and high-voltage situations to detect short-circuit faults.

REFERENCES

[1] J. Lin, Y. Hou, G. Zhu, S. Luo, P. Li, L. Qi, and L. Wang, "Co-optimization of unit commitment and transmission switching with short-circuit current constraints," in *Int. J. Electr. Power Energy Syst.*, vol. 110, pp. 309–317, Sep. 2019. doi: 10.1016/j.ijepes.2019.03.019.

[2] C. Huang, B. Zhang, Y. Ma, F. Zhou, and J. He, "Analysis of short-circuit current characteristics and its distribution of artificial grounding faults on DC transmission lines," *IEEE Trans. Power Del.*, vol. 33, no. 1, pp. 520–528, Feb. 2018. doi: 10.1109/TPWRD.2017.2732483.

[3] A. Heidary, H. Radmanesh, A. Bakhshi, K. Rouzbehi, and E. Pouresmaeil, "A compound current limiter and circuit breaker," *Electronics*, vol. 8, no. 5, p. 551, May 2019. doi: 10.3390/electronics8050551.

[4] S.-M. Song, J.-Y. Kim, S.-S. Choi, I.-D. Kim, and S. Choi, "New simple-structured AC solid-state circuit breaker," *IEEE Trans. Ind. Electron.*, vol. 65, no. 11, pp. 8455–8463, Nov. 2018. doi: 10.1109/TIE.2018.2809674.

[5] N. Huang, J. Qi, F. Li, D. Yang, G. Cai, G. Huang, J. Zheng, and Z. Li, "Short-circuit fault detection and classification using empirical wavelet transform and local energy for electric transmission line," *Sensors*, vol. 17, no. 9, p. 2133, Sep. 2017. doi: 10.3390/s17092133.

[6] T. S. Abdelgayed, W. G. Morsi, and T. S. Sidhu, "A new harmony search approach for optimal wavelets applied to fault classification," *IEEE Trans. Smart Grid*, vol. 9, no. 2, pp. 521–529, Mar. 2018. doi: 10.1109/TSG.2016.2555141.

[7] S. Sun, T. Du, B. Geng, C. Pang, M. Yu, and Y. Wang, "Research on the key accessory electrical parameter detection and test technology of frame type circuit breaker," *Electr. Meas. Instrum.*, vol. 53, no. 9, pp. 112–119, May 2016. doi: 10.3969/j.issn.1001-1390.2016.09.021.

[8] H. Chen, X. Liu, L. Li, Y. Liu, Y. Zhang, and Y. Huang, "Analysis of dynamic arc parameters for vacuum circuit breaker under short-circuit current breaking," *IEEE Trans. Appl. Supercond.*, vol. 29, no. 2, pp. 1–5, Mar. 2019, Art. no. 0601905. doi: 10.1109/TASC.2019.2891609.

[9] Z. Ya-Jun and C. Zhe, "The study of current sampling module based on intelligent tripping device," in *Proc. 9th Int. Conf. Fuzzy Syst. Knowl. Discovery*, Sichuan, China, 2012, pp. 1994–1997. doi: 10.1109/FSKD.2012.6234228.

[10] F. Yuan, B. Tang, C. Ding, S. Qin, L. Huang, and Z. Yuan, "Optimization design of a high-coupling split reactor in a parallel-type circuit breaker," *IEEE Access*, vol. 7, pp. 33473–33480, 2019. doi: 10.1109/ACCESS.2019.2900697.

[11] L. Yu, "Research on the intelligent releaser of high voltage circuit breaker based on Dsp (II): The part of software and hardware design," in *Proc. Int. Conf. Elect. Control Eng.*, Yichang, China, 2011, pp. 1236–1238. doi: 10.1109/ICECENG.2011.6057261.

[12] D. Feng, C. Weigang, M. Jiali, Z. Yue, and M. Anheuser, "One early short circuit current detection (ESCD) method based on the energy change," in *Proc. 27th Int. Conf. Elect. Contacts (ICEC)*, Dresden, Germany, 2014, pp. 1–4. [Online]. Available: http://ieeexplore.ieee.org/stamp/stamp.jsp?tp=&arnumber=6857222&isnumber=6857134.

[13] T. Mutzel, F. Berger, and M. Anheuser, "Methods of early short-circuit detection for low-voltage systems," in *Proc. 54th IEEE Holm Conf. Electr. Contacts*, Orlando, FL, USA, Oct. 2008, pp. 198–204. doi: 10.1109/HOLM.2008.ECP.44.

[14] L. Tan, "Low voltage air circuit breaker intelligent controller design and implementation," M.S. thesis, XATU, Xi'an, China, 2013.

[15] L.-A. Chen and P.-M. Zhang, "Early detection for short-circuit fault in low-voltage systems based on morphology-wavelet," *Proc. CSEE*, vol. 25, no. 10, pp. 24–28 and 88, May 2005. doi: 10.3321/j.issn:0258-8013.2005.10.005.

[16] X. Zheng and P. Zhang, "Fast opening control system of short-circuit faults based on dsPIC33F," *J. Fuzhou Univ.*, vol. 38, no. 6, pp. 850–855, Dec. 2010.

[17] X. Qin, P. Wang, Y. Liu, G. Sheng, and X. Jiang, "Research on distribution network fault recognition method based on time-frequency characteristics of fault waveforms," *IEEE Access*, vol. 6, pp. 7291–7300, 2018. doi: 10.1109/ACCESS.2017.2728015.

[18] H. Liang, Y. Chen, S. Liang, and C. Wang, "Fault detection of stator inter-turn short-circuit in PMSM on stator current and vibration signal," *Appl. Sci.*, vol. 8, no. 9, p. 1677, Sep. 2018. doi: 10.3390/app8091677.

[19] H.-C. Seo, "Novel protection scheme considering tie switch operation in an open-loop distribution system using wavelet transform," *Energies*, vol. 12, no. 9, p. 1725, May 2019. doi: 10.3390/en12091725.

[20] M.-F. Guo, N.-C. Yang, and L.-X. You, "Wavelet-transform based early detection method for short-circuit faults in power distribution networks," *Int. J. Elect. Power Energy Syst.*, vol. 99, pp. 706–721, Jul. 2018. doi: 10.1016/j.ijepes.2018.01.013.

[21] S. Mallat and S. Zhong, "Characterization of signals from multi-scale edges," *IEEE Trans. Pattern Anal. Mach. Intell.*, vol. 14, no. 7, pp. 710–732, Jul. 1992. doi: 10.1109/34.142909.

[22] L. Chen, P. Zhang, and X. Miao, "Prediction for the short-circuited fault based on wavelet transform," *Trans. China Electrotech. Soc.*, vol. 18, no. 2, pp. 91–94, Apr. 2003. doi: 10.3321/j.issn:1000-6753.2003.02.020.

[23] L. X. Wu and X. Miao, "Research on early detection of short-circuit fault in multi-level low voltage system," *Adv. Technol. Elect. Eng. Energy*, vol. 34, no. 9, pp. 38–43, Sep. 2015. doi: 10.3969/j.issn.1003-3076.2015.09.007.

[24] C. Li'an and P. Zhang, "Research on threshold of early prediction for short circuit fault based on wavelet transform," *Trans. China Electrotech. Soc.*, vol. 20, no. 3, pp. 64–69, Mar. 2005. doi: 10.3321/j.issn:1000-6753.2005.03.012.

[25] X.-G. Xia, C.-C. J. Kuo, and Z. Zhang, "Wavelet coefficient computation with optimal prefiltering," *IEEE Trans. Signal Process.*, vol. 42, no. 8, pp. 2191–2197, Aug. 1994. doi: 10.1109/78.301858.

GUANGHAI BAO received the B.S. and Ph.D. degrees in electrical engineering from Fuzhou University, Fujian, China, in 2000 and 2011, respectively. He held a postdoctoral position with Changshu Switching Manufacturing Company Ltd. He is currently an Associate Professor and the Department Head of the College of Electronic Science and Engineering, Fuzhou University. His research interests mainly include electrical appliances and fault diagnosis.

FENG ZENG received the B.S. degree from Minnan Normal University, Fujian, China, in 2017, where he is currently pursuing the master's degree. His main research interests include the detection of short-circuit faults and leakage current.

HUAIPING SUN received the B.S. and M.S. degrees from Fuzhou University, Fujian, China, in 2015 and 2018, respectively. He is currently with the Nanan Power Supply Bureau of State Grid, Fujian. His main research interest includes the detection of short-circuit faults.